

Adenylyl cyclase/cAMP system involvement in the antiangiogenic effect of somatostatin in the retina. Results from transgenic mice.

Chiara Ristori¹, Maria Enrica Ferretti², Barbara Pavan², Franco Cervellati², Giovanni Casini³, Elisabetta Catalani³, Massimo Dal Monte¹, Carla Biondi².

¹Dipartimento di Biologia - Università di Pisa - Pisa, Italy

²Dipartimento di Biologia ed Evoluzione - Università di Ferrara - Ferrara, Italy.

³Dipartimento di Scienze Ambientali - Università della Tuscia - Viterbo, Italy.

Running head: Involvement of AC system in SRIF antiangiogenic action in hypoxic mouse retina.

Corresponding author: Carla Biondi, Dipartimento di Biologia ed Evoluzione – Università di Ferrara – Via L. Borsari, 46 – 44100 Ferrara, Italy – Phone: +39 0532 455482 – FAX: +39 0532 207143 – e-mail: clm@unife.it

Abstract

Neoangiogenesis is a response to retinal hypoxia that is inhibited by somatostatin (SRIF) through its subtype 2 receptor (sst2). Using a mouse model of hypoxia-induced retinopathy, we investigated the possibility that inhibition of adenylyl cyclase (AC) is involved in SRIF anti-angiogenic actions. Hypoxia increased AC responsiveness in wild type (WT) retinas and in retinas lacking sst2, but not in sst2-overexpressing retinas. Hypoxia also altered AC isoform expression, but with different patterns depending on sst2 expression level. Among the nine AC isoforms, AC VII isoform mRNA and protein resulted the most affected. Indeed, in hypoxia AC VII expression was significantly enhanced in WT retinas and it was further increased in sst2-lacking retinas, but not in retinas overexpressing sst2. These data suggest an involvement of AC/cAMP in mediating both hypoxia-evoked retinal neoangiogenesis and SRIF protective actions. The AC VII isoform is a candidate to a main role in these mechanisms.

Key words: somatostatin; adenylyl cyclase system; hypoxia; mouse retina; transgenic mice.

Introduction

Proliferative retinopathy is characterized by the generation of proangiogenic factors resulting in excessive proliferation of new blood vessels within the retina [1,2]. Other molecules, acting as antiangiogenic factors, can regulate the angiogenic process [1]. Several lines of experimental and clinical evidence indicate that somatostatin (SRIF) and its analogues may act as antiangiogenic factors [3-7].

Although the mechanisms underlying SRIF antiangiogenic actions remain to be elucidated, it has been proposed that this peptide acts both directly, by inhibiting endothelial cell proliferation, and indirectly through a reduction of the release of proangiogenic factors, such as vascular endothelial growth factor (VEGF) [8-10].

SRIF binds to five different subtypes of heterotrimeric G-protein coupled receptors, which have been cloned and termed sst1 through sst5 [11]. The transduction pathways influenced by SRIF receptors have been poorly characterized in mammalian retinas, however an inhibition of adenylyl cyclase (AC) activity by SRIF has been described in the mouse retina [12], indicating that retinal pathways activated by SRIF are likely to be the same as those of other nervous or non-nervous tissues. Indeed, although each receptor subtype can influence different signal transduction pathways, all five receptors are functionally coupled to AC inhibition [13] leading to a reduction of intracellular adenosine 3',5'cyclic AMP (cAMP).

Nine AC isoforms (AC I-IX) have been cloned [14] and all, with the exception of AC VII, have been reported in mammalian retinas [15,16]. Taken together, these observations indicate that AC inhibition may be implicated in SRIF antiangiogenic actions in the retina. Consistently, activation of cAMP pathway has been reported to result in proangiogenic effects in a variety of experimental models [17-20].

Among SRIF receptors, sst2 is likely to be responsible for SRIF antiangiogenic actions in the retina. Indeed, sst2 preferring agonists inhibit neovascularization in proliferative

diabetic retinopathy [6,7] and counteract growth factor-induced proliferation of bovine retinal endothelial cells under hypoxic conditions [3].

We have recently employed transgenic mice to investigate the involvement of sst2 in mediating SRIF antiangiogenic actions. In particular, sst1 knockout (KO) mice are a model of sst2 overexpression [22-24], while sst2 KO mice are a model of null sst2 expression. Using retinas from these mice in a model of hypoxia-induced retinopathy, we have demonstrated that neovascularization and VEGF expression significantly increase in the absence of sst2 [21], while VEGF expression is significantly reduced when sst2 is overexpressed [21]. In the present work, using sst1 or sst2 KO mice and the model of hypoxia-induced retinopathy, we investigated the hypothesis of a correlation between sst2 expression, AC activity and AC isoform expression, supporting a role for the AC/cAMP system in mediating SRIF antiangiogenic effects through sst2.

Experimental Procedure

Animals

Experiments were performed on retinas from normoxic and hypoxic mice of WT (C57BL/6) and sst1 or sst2 KO strains of both sexes. sst1 and sst2 KO mice were generated as previously reported [25,26]. Hypoxic mice were obtained utilizing the hypoxia-induced retinopathy model described by Smith et al. [27]. Briefly, the model was produced in newborn mouse pups at postnatal day (PD)7 by exposure to 75% oxygen for five days and subsequent recovery in a room-air environment. After the transfer of pups to a normoxic condition (PD 12), the developing relative retinal hypoxia led to induction of abnormal vasoproliferation that reached a maximum at PD 17. Mice kept in room air were used as controls (normoxia). At PD

17, normoxic and hypoxic mice were sacrificed and retinas were dissected, as described [21]. Mice were nursed in the animal house of the Department of Biology at the University of Pisa and maintained in controlled environment with food and water ad libitum. All the animal studies were performed according to the guidelines and approval of the ARVO Statement for the Use of Animals in Ophthalmic and Vision Research and in compliance with the Italian law on animal care N°116/1992 and the EEC/609/86. All efforts were made to reduce the number of animals used.

Membrane preparations

Normoxic and hypoxic retinas, dissected from WT and transgenic mice at PD 17, were teased from the pigment epithelium and maintained in ice-cold buffer (10 mM Hepes/Tris, 10% sucrose, pH 7.4). Retinas (12 per vial) were then frozen in liquid nitrogen and stored at -80°C. The thawed retinas were homogenized using a Dounce homogenizer in the same ice-cold buffer. The homogenate was centrifuged at 1,000 *g* for 10 min, the supernatant was aspirated and stored. The pellet was re-suspended, re-homogenized, and centrifuged as above. The two supernatants were combined and centrifuged at 11,000 *g* for 20 min. The pellet was re-suspended in 30 ml of ice-cold buffer without sucrose and centrifuged at 27,000 *g* for 10 min. Finally, the pellet was re-suspended in the same buffer supplemented with the protease inhibitors aprotinin (20 µg/ml) and leupeptin (20 µg/ml) and used immediately. All steps of the above procedure were performed at 4°C. Protein concentration was determined according to Bradford [28], using bovine serum albumin as a standard.

Measurements of AC activity

AC activity was measured as previously reported [12]. Briefly, the standard assay

mixture (0.4 ml/tube) contained: 75 mM Hepes/Tris, 1 mM MgSO_4 , 10 μM 3-isobutyl-1-methylxanthine (IBMX), 500 μM GTP, 1 mM EGTA, pH 7.4, plus 50 μg of membrane protein/tube and test substances, when indicated. Membranes were preincubated for 20 min at 0°C, the reaction was then initiated by the addition of 500 μM ATP, carried out for 10 min at 30°C and stopped by 2 min of boiling. After centrifugation of samples, cAMP was measured on the clear supernatant, according to the method of Brown et al. [29]. Each experiment was performed in duplicate. The data were expressed as pmol cAMP/mg protein/10 min.

RNA preparation, cDNA synthesis, and real time PCR analysis

Total RNA was extracted from 6 retinas of PD 17 normoxic and hypoxic WT and KO mice, using the RNeasy Mini Kit (Qiagen, Valencia, CA), according to the manufacturer's recommended procedure. RNA samples were treated with DNase to remove traces of genomic DNA, solubilized in RNase-free water and quantified by spectrophotometric analysis. The samples were checked for integrity using formaldehyde denaturing RNA gel electrophoresis (1.2%) before proceeding with the further real time PCR analysis. cDNA synthesis was performed with 1 μg of total RNA using iScript cDNA Synthesis Kit (Bio-Rad, Hercules, CA, USA) in a final volume of 20 μl , according to the manufacturer's protocol. Real time PCR was performed using SYBR Green on MiniOpticon System (Bio-Rad). The final reaction mixture contained 1 μl of cDNA, 300 nM of each primer, 7.5 μl of iQ SYBR green Supermix (Bio-Rad), and RNase-free water to complete the reaction mixture volume to 15 μl . Primer sequences are shown in Table I. Negative control reactions were set up as above without any template cDNA. All reactions were run as triplicates. The PCR was performed with hot-start denaturation step at 95°C for 3 min, and then was carried out for 40 cycles at 95°C for 10 sec and 58°C for 20 sec. The fluorescence was read during the reaction, allowing a continuous monitoring of the amount of PCR product. Dissociation curve analysis was performed for

quality control with data collection from a subsequent temperature ramp from 65°C to 95°C. Real time PCR products were analyzed on a GelStar (Cambrex, East Rutherford, NJ)-containing 3% agarose gel to verify the correct product sizes. Products identity was confirmed by automated DNA sequencing (ABI PRISM 3130 Applied Biosystems). The efficiency of target amplification had values close to 100% for all primer combinations. The comparative Ct (threshold cycle) method normalized to cyclophilin B, a stable mRNA in our experimental conditions, was used to analyze relative changes in gene expression as previously described (amount of target = $2^{-\Delta\Delta C_t}$) [32].

Immunohistochemistry

The eyes were removed from normoxic and hypoxic WT and KO animals at PD 17 and immersion fixed in 2% paraformaldehyde in 0.1 M phosphate buffer (PB), pH 7.4, for 2 h. The fixed eyes were transferred to 25% sucrose in 0.1 M PB and stored at 4°C. The retinas were cut with the whole eye in a plane perpendicular to the vitreal surface at 10 µm with a cryostat. The sections were mounted onto gelatin-coated slides and stored at -20°C. For immunohistochemical detection of AC VII, sections from normoxic as well as hypoxic WT and KO retinas were washed in 0.1 M PB and incubated overnight at 4°C in AC VII antibodies (sc-25501) diluted 1:400 in 0.1 M PB containing 1% Triton X-100. Following washes in 0.1 M PB, the sections were incubated in secondary antibody conjugated with Alexa Fluor 546 at a dilution of 1:200 in 0.1 M PB containing 0.5% Triton X-100 for 1-2 hours at room temperature (RT). Then, the slides were coverslipped in a 0.1 M PB-glycerin mixture. In control experiments, where the primary antibody was omitted, no unspecific staining was observed in any retinal layer. Immunofluorescence images were acquired with a laser confocal scanning microscope (Leica Microsystems Heidelberg GmbH, Mannheim,

Germany). The digital images were sized and saved at a minimum of 300 dpi using Adobe Photoshop (Adobe Systems, Mountain View, CA).

Statistical analysis

Data were examined by unpaired *t* test or ANOVA, followed by Dunnett's comparison post test, as appropriate. Differences were considered statistically significant at $p < 0.05$. The software PRISM (version 4.0, Graph Pad Software Inc., San Diego, CA) was used. All data are reported as means \pm SEM.

Chemicals

[8-³H]adenosine 3'-5'-cyclic phosphate (specific activity 24 Ci/mmol) was from Amersham Biosciences, GE Healthcare UK Ltd, Little Chalfont, England. Aprotinin, leupeptin, IBMX, GTP, cAMP, ATP, EGTA, FSK, SRIF and epinephrine were from Sigma, St. Louis, MO. Octreotide (OCTR) was provided from Novartis, Basel, Switzerland. AC VII antibody (sc-25501) was from Santa Cruz Biotechnology, Santa Cruz, CA. Secondary antibody conjugated with Alexa Fluor 546 was from Molecular Probes, Eugene, OR.

Results

Adenylyl cyclase activity

AC activity measured on membrane preparations is reported in Table II. In normoxic retinas, AC basal activity was similar in WT and *sst1* KO, but it was significantly reduced in *sst2* KO retinas (-21%). The enzyme was potently stimulated by FSK and it was also activated

by epinephrine, whose receptors, positively coupled to AC, are expressed in the rodent retina [33]. FSK-stimulated AC activity was insensitive to SRIF or OCTR in WT and in *sst2* KO retinas while, as expected [12], SRIF or OCTR greatly reduced FSK-stimulated AC activity (-47% and -51%, respectively) in *sst1* KO retinas. FSK and epinephrine concentration (1 μ M) was chosen on the basis of dose-response curves (data not shown). SRIF and OCTR were utilized at 1 μ M, according to our previous results [12]. Overall, the observations in normoxic retinas were in agreement with those reported by Pavan et al. [12].

In hypoxic retinas, AC basal activity was significantly enhanced with respect to normoxic in *sst2* KO retinas (+65%). In addition, the enzyme responsiveness to FSK and epinephrine was significantly increased both in WT (+26%, +34%, respectively) and in *sst2* KO (+90%, +158%, respectively), but not in *sst1* KO retinas. Similar to normoxic, also in hypoxic retinas SRIF or OCTR did not affect FSK-stimulated AC activity in WT or in *sst2* KO retinas. In contrast, in *sst1* KO hypoxic retinas both SRIF and OCTR greatly decreased FSK-stimulated AC activity (-48%, -56%, respectively) and the recorded values were not different from those in normoxic retinas.

In summary, the hypoxic treatment caused a massive increase of FSK- or epinephrine-stimulated AC activity both in WT and in *sst2* KO retinas. In addition, in these retinas FSK-stimulated AC activity was not influenced by either SRIF or OCTR. In contrast, FSK- or epinephrine-stimulated AC activity in *sst1* KO retinas subjected to hypoxic treatment tended to remain similar to that in normoxic retinas, and the inhibition of the FSK-stimulated AC activity by SRIF or OCTR persisted.

Adenylyl cyclase isoform mRNA expression

In order to find possible correlates of AC activity changes in the different experimental conditions described above, a real time PCR analysis was performed to determine the

expression levels of AC isoforms in normoxic and in hypoxic mouse retinas. Preliminary experiments performed on PD 17 WT normoxic mice showed that all AC isoform (AC I-IX) transcripts are expressed in the retina (Fig. 1).

The relative levels of all transcripts in normoxic and hypoxic conditions normalized to cyclophilin B were evaluated (Fig. 2). As shown in Fig. 2A, in normoxic retinas the genetic deletion of *sst1* did not alter AC isoform expression pattern versus WT. In contrast, when compared to WT, in *sst2* KO retinas a statistically significant reduction of the mRNAs for some AC isoforms (AC II, III, VI and IX, -29%, -37%, -43%, -40%, respectively) was detected.

The analysis of retinas in hypoxic conditions (Fig. 2B) revealed a significantly different expression pattern of AC isoforms. In particular, in WT retinas mRNA expression of AC II, III and V significantly decreased (-25%, -27%, -28%, respectively), whereas AC VII mRNA expression highly increased (+103%) with respect to normoxic retinas. In *sst1* KO retinas, AC III and IX mRNAs significantly decreased (-30% and -27%, respectively), whereas AC VII and VIII mRNA expression significantly increased (+41% and +38%, respectively). In *sst2* KO retinas, AC V mRNA underwent a statistically significant decrease (-24%), whereas a statistically significant increase of mRNAs for AC I, VI, VII and VIII was observed (+41%, +48%, +169%, and +34%, respectively).

In summary, the hypoxic treatment induced significant changes in the pattern of AC isoform expression in the retinas of all three mouse strains. The most apparent modifications were at the level of AC VII, whose expression was greatly increased in all strains, although the enhancement in *sst1* KO retinas was significantly (?) less marked than in WT or in *sst2* KO retinas.

Immunohistochemistry

As shown by the real time PCR results, the AC VII isoform appears to be the most affected by hypoxic treatment. This AC isoform has not been reported previously in mammalian retinas, therefore we performed an immunohistochemical analysis to localize this AC isoform and support the real time PCR data. In addition, although immunohistochemistry is not a reliable quantitative technique, we checked whether the hypoxia-induced alterations could be observed in immunostained retinal sections.

As shown in Fig. 3A, the pattern of AC VII immunofluorescence in normoxic WT retinas was characterized by punctate staining, which was mainly confined to the photoreceptor outer segments, the outer plexiform layer (OPL), the inner plexiform layer and the ganglion cell layer. Similar patterns of AC VII immunoreactivity could be observed in normoxic *sst1* KO and *sst2* KO retinas. However, as shown in Fig. 3B-D, these patterns appeared to be differentially affected by hypoxic treatment. Indeed, a slight but evident increase of AC VII immunofluorescence intensity was observed in hypoxic WT retinas with respect to their normoxic controls, particularly in the OPL (Fig. 3B). In contrast, no apparent differences were detected between normoxic and hypoxic *sst1* KO retinas (Fig. 3C). Finally, in *sst2* KO retinas a considerable increase of AC VII immunofluorescence intensity could be seen after hypoxic treatment in all retinal layers containing AC immunoreactivity (Fig. 3D).

Together, these changes in AC VII immunofluorescence were in line with those in AC VII mRNA expression observed with real time PCR.

Discussion

In the present study, we have provided evidence of correlations between hypoxic conditions, levels of *sst2* expression and alterations of the AC/cAMP system, suggesting an involvement of this transduction pathway in *sst2*-mediated antiangiogenic actions of SRIF.

These data also confirm and expand previous studies regarding AC/cAMP system modulation by SRIF and in the mouse retina [12].

In addition to WT retinas, we have utilized retinas from transgenic mice where *sst2* is either overexpressed and overfunctional (the *sst1* KO retinas) [12,23], or absent (the *sst2* KO retinas). These genetically modified strains represent useful experimental models to investigate the role of such receptor in mediating SRIF responses. A central part of our study has been concerned with measurements of AC activity in response to SRIF or OCTR. To detect the effects of these substances, AC was stimulated by FSK. Indeed, as previously reported in the retina as well as in other different tissues, SRIF effects on AC activity become well evident when this activity is sustained by stimulators, among which FSK [12,34,35].

SRIF and the AC/cAMP system in normoxic retinas

The data of AC activity in normoxic retinas are in line with those of our previous studies [12]. Basal AC activity was similar in WT and *sst1* KO retinas, whereas a reduction was observed in *sst2* KO retinas. AC responsiveness to stimulators such as FSK or epinephrine was similar in all strains, however AC inhibition by SRIF or OCTR was only observed in *sst1* KO retinas. As previously reported, this effect is likely to be due to a better coupling between *sst2* and G α_o , since both *sst2* and G protein expressions are increased in *sst1* KO retinas [12,23].

Our data show that the mRNAs of all nine AC isoforms are present in the different strains, however AC VII isoform has not been reported previously in mammalian retinas [15,16]. The lack of evidence of AC VII mRNA in previous studies may be due to different species used as experimental models, or to different experimental protocols. To our knowledge, this is the first report of AC VII in the mouse retina both at the mRNA and at the protein level, which substantiates the presence of AC VII in the mouse retina.

The AC mRNA expression patterns were not different in sst1 KO with respect to WT retinas, whereas a reduction of expression was evident for several AC isoform mRNAs in sst2 KO retinas. These results indicate that the pattern of AC isoform expression is highly influenced by sst2 deletion, but not sst1 deletion with consequent sst2 overexpression. At present, it is difficult to explain why an alteration of sst expression results in a change of the availability of AC system components. Our previous observations showed an increased expression of Gao in mouse retinas with sst1 deletion [12]. In addition, it has been clearly demonstrated that an altered functionality of Gai/o-coupled receptors, sst included, may induce modifications of the expression of various AC transduction system components, including catalytic subunits [36]. The decreased expression of some AC isoforms in sst2 KO retinas may explain the decrease of enzyme basal activity with respect to WT retinas.

SRIF and the AC/cAMP system in hypoxic retinas

Concerning the data on AC activity in hypoxic conditions, the most evident finding is that the hypoxic treatment significantly increased AC responsiveness to FSK and epinephrine in WT and in sst2 KO retinas. In the latter, an enhancement of the enzyme activity was also evident in basal conditions. It is important to note that, in contrast, stimulated AC activity was not significantly affected in the presence of sst2 overexpression, as in sst1 KO retinas. Moreover, while SRIF or OCTR treatment was ineffective in WT or in sst2 KO retinas, it decreased AC activity in sst1 KO retinas to levels that were not significantly different from those measured in similarly treated sst1 KO normoxic retinas. Together, these observations indicate that overexpression of sst2, as in sst1 KO retinas, counteracts the effects of hypoxia on AC activity, while lack of sst2 amplifies these effects.

The analysis of AC isoform mRNA expression in hypoxic WT retinas showed a decrease of AC II, III, and V expression, but a great enhancement of AC VII mRNA with

respect to normoxic WT retinas. Alterations of AC isoform expression in response to oxygen deficiency have been observed in different tissues [37,38]. In *sst1* or *sst2* KO retinas, the combination of hypoxia and *sst2* expression level resulted in strain-specific changes. Noteworthy, AC VII mRNA expression increased in all strains, but to a lesser extent in *sst1* KO and to a higher extent in *sst2* KO retinas, if compared to the enhancement in WT. These changes in AC VII mRNA expression were substantiated by our immunofluorescence data showing concordant variations in immunofluorescence intensity. At present we have no plausible explanation for these changes observed in *sst1* and *sst2* KO retinas in hypoxic conditions. However, further alterations of *sst2* expression can be excluded, since we previously demonstrated that hypoxia does not alter *per se* *sst2* expression [21].

It has been demonstrated that the AC VII isoform is highly responsive to stimulatory agents, and insensitive to all known inhibitory regulators, *Gai/o* included [39]. Therefore, its enhanced expression could be mostly responsible for the observed *in vitro* increase in AC responsiveness to stimulators. Since it has been reported that hypoxia increases the release of AC stimulatory agents, such as catecholamines and adenosine, as well as their receptor expression [40-42], AC VII isoform may play a central role in the enhancement of cAMP in these conditions.

The increased cAMP level in hypoxia is likely to be instrumental to the induction of neoangiogenesis and the increased expression of proangiogenic factors such as VEGF, that we have observed recently in all three strains, in the same experimental model. In particular, compared to WT retinas, both angiogenesis and VEGF expression are increased in *sst2* KO, while VEGF expression is decreased in *sst1* KO retinas [21]. Together, these findings suggest that an enhanced somatostatinergic function at *sst2* protects against the production of proangiogenic cAMP, while *sst2* deletion results in an opposite condition.

Conclusion

In conclusion, we have investigated the AC/cAMP transduction pathway in an *in vivo* model of retinal hypoxia using retinas from WT mice and from mice with over- or null sst2 expression. We observed changes of both AC activity and expression in response to hypoxia. Most importantly, these changes could be correlated with different levels of sst2 expression, as the patterns of AC activity or AC isoform expression were different in WT, sst1 KO or sst2 KO retinas. These data provide evidence in support of an involvement of the AC/cAMP system in mediating not only hypoxia-evoked retinal neoangiogenesis, but also SRIF protective actions. The AC VII isoform is a candidate to a main role in these mechanisms.

Acknowledgements

This work was supported by the Italian Ministry of University and Research (MUR, PRIN, grant 2005052312) and the Fondazione Cassa di Risparmio di Cento.

We thank G. Bertolini (University of Pisa, Italy) for assistance with mouse colonies.

References

1. Campochiaro PA (2004) Ocular neovascularisation and excessive vascular permeability. *Expert Opin Biol Ther* 4:1395-1402
2. Gariano RF, Gardner TW (2005) Retinal angiogenesis in development and disease. *Nature* 438:960-966
3. Baldysiak-Figiel A, Lang GK, Kampmeier J et al (2004) Octreotide prevents growth factor-induced proliferation of bovine retinal endothelial cells under hypoxia. *J Endocrinol* 180:417-424
4. Grant MB, Mames RN, Fitzgerald C et al (2000) The efficacy of octreotide in the therapy of severe nonproliferative and early proliferative diabetic retinopathy: a randomized controlled study. *Diabetes Care* 23:504-509
5. Simo R, Lecube A, Sararols L et al (2002) Deficit of somatostatin-like immunoreactivity in the vitreous fluid of diabetic patients: possible role in the development of proliferative diabetic retinopathy. *Diabetes Care* 25:2282-2286
6. Davis MI, Wilson SH, Grant MB (2001) The therapeutic problem of proliferative diabetic retinopathy: targeting somatostatin receptors. *Horm Metab Res* 33:295-299
7. Grant MB, Caballero S (2002) Somatostatin analogues as drug therapies for retinopathies. *Drugs Today* 38:783-791
8. Garcia de la Torre N, Wass JA, Turner HE (2002) Antiangiogenic effects of somatostatin analogues. *Clin Endocrinol* 57:425-441
9. Sall JW, Klisovic DD, O'Dorisio MS et al (2004) Somatostatin inhibits IGF-1 mediated induction of VEGF in human retinal pigment epithelial cells. *Exp Eye Res* 79:465-476
10. Dasgupta P (2004) Somatostatin analogues: multiple roles in cellular proliferation,

- neoplasia, and angiogenesis. *Pharmacol Ther* 102:61-85
11. Weckbecker G, Lewis I, Albert R et al (2003) Opportunities in somatostatin research: biological, chemical and therapeutic aspects. *Nat Rev Drug Discov* 2:999-1017
 12. Pavan B, Fiorini S, Dal Monte M et al (2004) Somatostatin coupling to adenylyl cyclase activity in the mouse retina. *Naunyn-Schmiedebergs Arch Pharmacol* 370:91-98
 13. Olias G, Viollet C, Kusserow H et al (2004) Regulation and function of somatostatin receptors. *J Neurochem* 89:1057-1091
 14. Hanoune J, Defer N (2001) Regulation and role of adenylyl cyclase isoforms. *Annu Rev Pharmacol Toxicol* 41:145-174
 15. Beitz E, Volkel H, Guo Y et al (1998) Adenylyl cyclase type 7 is the predominant isoform in the bovine retinal pigment epithelium. *Acta Anat* 162:157-162
 16. Abdel-Majid RM, Tremblay F, Baldridge WH (2002) Localization of adenylyl cyclase proteins in the rodent retina. *Brain Res Mol Brain Res* 101:62-70
 17. Amano H, Ando K, Minamida S et al (2001) Adenylate cyclase/protein kinase A signaling pathway enhances angiogenesis through induction of vascular endothelial growth factor in vivo. *Jpn J Pharmacol* 87:181-188
 18. Sakurai S, Alam S, Pagan-Mercado G et al (2002) Retinal capillary pericyte proliferation and c-Fos mRNA induction by prostaglandin D2 through the cAMP response element. *Invest Ophthalmol Vis Sci* 43:2774-2781
 19. Casibang M, Purdom S, Jakowlew S et al (2001) Prostaglandin E2 and vasoactive intestinal peptide increase vascular endothelial cell growth factor mRNAs in lung cancer cells. *Lung Cancer* 31:203-212
 20. Schwarz N, Renshaw D, Kapas S et al (2006) Adrenomedullin increases the expression of calcitonin-like receptor and receptor activity modifying protein 2 mRNA

- in human microvascular endothelial cells. *J Endocrinol* 190:505-514
21. Dal Monte M, Cammalleri M, Martini D et al (2007) Anti-angiogenic role of somatostatin receptor 2 in a model of hypoxia-induced neovascularization in the retina: results from transgenic mice. *Invest Ophthalmol Vis Sci* 48:3480-3489
 22. Dal Monte M, Petrucci C, Cozzi A et al (2003) Somatostatin inhibits potassium evoked glutamate release by activation of the sst2 somatostatin receptor in the mouse retina. *Naunyn-Schmiedeberg Arch Pharmacol* 367:188-192
 23. Dal Monte M, Petrucci C, Vasilaki A et al (2003) Genetic deletion of somatostatin receptor 1 alters somatostatinergic transmission in the mouse retina. *Neuropharmacology* 45:1080-1092
 24. Casini G, Dal Monte M, Petrucci C et al (2004) Altered morphology of rod bipolar cell axonal terminals in the retinas of mice carrying genetic deletion of somatostatin subtype receptor 1 or 2. *Eur J Neurosci* 19:43-54
 25. Kreienkamp HJ, Akgun E, Baumeister H et al (1999) Somatostatin receptor subtype 1 modulates basal inhibition of growth hormone release in somatotrophs. *FEBS Lett* 462:464-466
 26. Allen JP, Hathway GJ, Clarke NJ et al (2003) Somatostatin receptor 2 knockout/lacZ knockin mice show impaired motor coordination and reveal sites of somatostatin action within the striatum. *Eur J Neurosci* 17:1881-1895
 27. Smith LE, Wesolowski E, McLellan A et al (1994) Oxygen-induced retinopathy in the mouse. *Invest Ophthalmol Vis Sci* 35:101-111
 28. Bradford MM (1976) A rapid and sensitive method for the quantitation of microgram quantities of protein utilizing the principle of protein-dye binding. *Anal Biochem* 72:248-254
 29. Brown BL, Ekins RP, Albano JD (1972) Saturation assay for cyclic AMP using

- endogenous binding protein. *Adv Cyclic Nucleotide Res* 2:25-40
30. Wang X, Seed B (2003) A PCR primer bank for quantitative gene expression analysis. *Nucleic Acids Res* 31:e154
 31. Rozen S, Skaletsky H (2000) Primer3 on the WWW for general users and for biologist programmers. *Methods Mol Biol* 132:365-386
 32. Livak KJ, Schmittgen TD (2001) Analysis of relative gene expression data using real-time quantitative PCR and the 2(-Delta Delta C(T)) method. *Methods* 25:402-408.
 33. Tsai WH, Koh SW, Puro DG (1987) Epinephrine regulates cholinergic transmission mediated by rat retinal neurons in culture. *Neuroscience* 22:675-680
 34. Colas B, Valencia AM, Prieto JC et al (1992) Somatostatin binding and modulation of adenylate cyclase in ovine retina membranes. *Mol Cell Endocrinol* 88:111-117
 35. Masmoudi O, Gandolfo P, Tokay T et al (2005) Somatostatin down-regulates the expression and release of endozepines from cultured rat astrocytes via distinct receptor subtypes. *J Neurochem* 94:561-571
 36. Watts VJ, Neve KA (2005) Sensitization of adenylate cyclase by Galpha i/o-coupled receptors. *Pharmacol Ther* 106:405-421
 37. Takeo S, Niimura M, Miyake-Takagi K et al (2003) A possible mechanism for improvement by a cognition-enhancer nefiracetam of spatial memory function and cAMP-mediated signal transduction system in sustained cerebral ischaemia in rats. *Br J Pharmacol* 138:642-654
 38. Zhao Y, Xu D, Quaegebeur JM et al (2002) Expression of adenylyl cyclase V/VI mRNA and protein is upregulated in cyanotic infant human myocardium. *Pediatr Cardiol* 23:536-541.
 39. Cooper DM, Crossthwaite AJ (2006) Higher-order organization and regulation of adenylyl cyclases. *Trends Pharmacol Sci* 27:426-431

40. Palmer GC (1985) Cyclic nucleotides in stroke and related cerebrovascular disorders. Life Sci 36:1995-2006
41. Rocha-Singh KJ, Honbo NY, Karliner JS (1991) Hypoxia and glucose independently regulate the beta-adrenergic receptor-adenylate cyclase system in cardiac myocytes. J Clin Invest 88:204-213
42. Kuroko Y, Yamazaki T, Tokunaga N et al (2007) Cardiac epinephrine synthesis and ischemia-induced myocardial epinephrine release. Cardiovasc Res 74:438-444

Captions to the Figures

Fig. 1. AC isoform mRNA expression in PD 17 WT normoxic retinas. Total RNA was extracted from the retinas, reverse transcribed, and real time PCR performed with isoform-specific primers as described in Materials and Methods. M: DNA Marker 50 bp ladder; Lane 1: AC type I; Lane 2: AC type II; Lane 3: AC type III; Lane 4: AC type IV; Lane 5: AC type V; Lane 6: AC type VI; Lane 7: AC type VII; Lane 8: AC type VIII; Lane 9: AC type IX.

Fig. 2. AC isoform mRNA expression by real time PCR in WT (white bars), *sst1* KO (black bars) and *sst2* KO (grey bars) mouse retinas.

A: AC isoforms expression level in normoxic conditions Each panel shows the ratio between optical density (OD) of AC mRNA isoform and cyclophilin B mRNA in normoxic (white bar) and hypoxic (black bar) retinas from the three mouse strains. Representative agarose gel electrophoresis of PCR for AC isoforms and relative control loading cyclophilin B (Cyc) amplicons is shown in the top of each panel. Data are means \pm SEM of at least six independent experiments. ° $p < 0.05$ vs WT normoxic (ANOVA, followed by Dunnett's post test); * $p < 0.05$ vs relative normoxic condition (unpaired t test); § $p < 0.05$ vs WT hypoxic (ANOVA, followed by Dunnett's post test).

Fig. 3. A: pattern of AC VII immunofluorescence in a WT, normoxic mouse retina. punctate immunolabeling was densely distributed to the photoreceptor outer segments (POS) and it was evident in the outer plexiform layer (OPL), in the inner plexiform layer (IPL) and in the ganglion cell layer (GCL). B-D: AC VII immunostaining patterns in WT (B), *sst1* KO (C) and *sst2* KO (D) retinas in normoxic (left half of each panel) or in hypoxic (right half of each panel) conditions. A detectable increase of immunofluorescence intensity can be appreciated

after hypoxic treatment in WT retinas; no changes are seen in sst1 KO retinas; an evident increase is seen in sst2 KO retinas. All images are single confocal optical sections. INL, inner nuclear layer; ONL, outer nuclear layer. Scale bars: 20 μm .

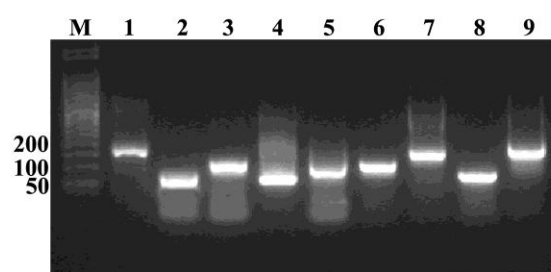


Fig.1

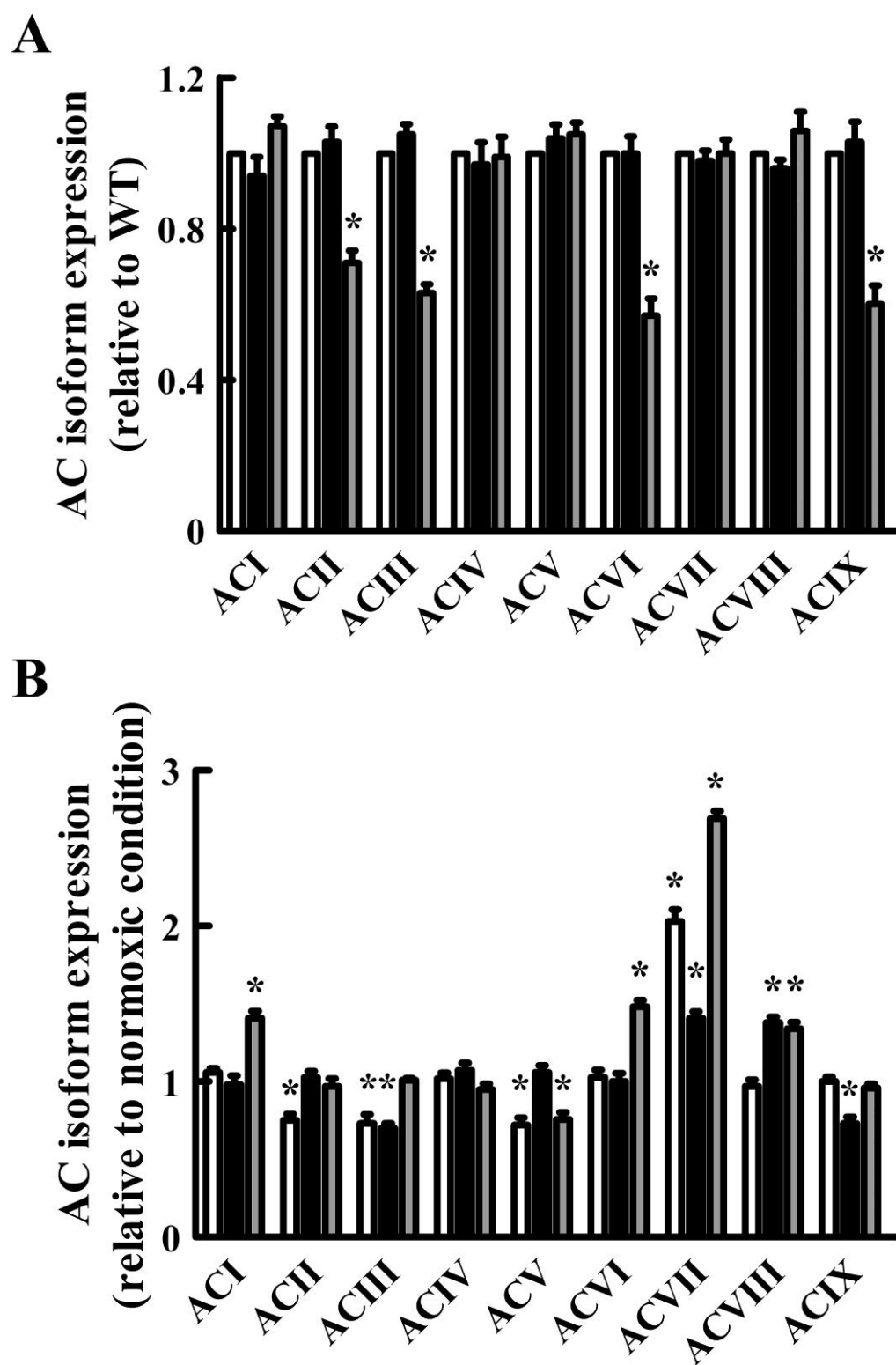


Fig.2

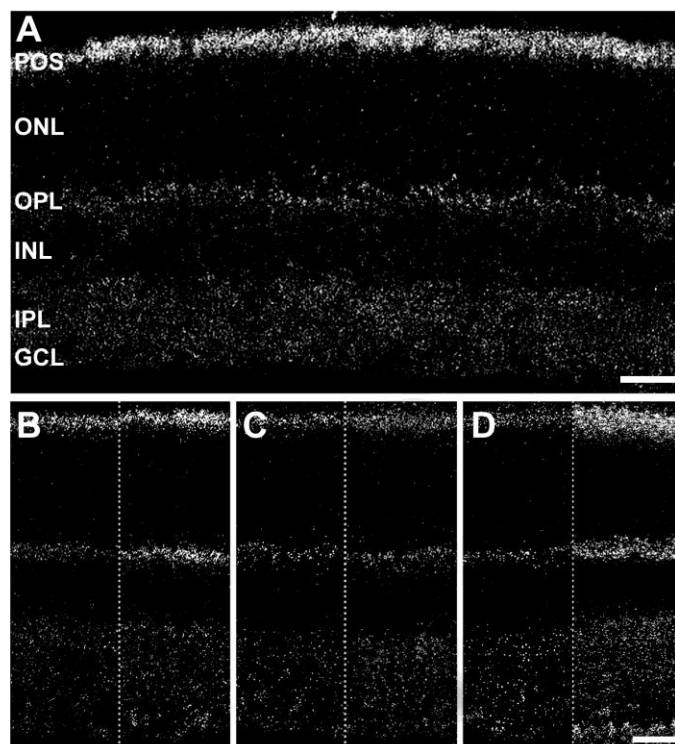


Fig.3